ARTICLE

Uptake and Intracellular Fate of Disulfide-Bonded Polymer Hydrogel Capsules for Doxorubicin Delivery to Colorectal Cancer Cells

Yan Yan,[†] Angus P. R. Johnston,[†] Sarah J. Dodds,[†] Marloes M. J. Kamphuis,[†] Charles Ferguson,[‡] Robert G. Parton,[‡] Edouard C. Nice,[§] Joan K. Heath,[§,#,*] and Frank Caruso[†,#,*]

[†]Centre for Nanoscience and Nanotechnology, Department of Chemical and Biomolecular Engineering, The University of Melbourne, Victoria 3010, Australia, [‡]Institute for Molecular Bioscience and Centre for Microscopy and Microanalysis, The University of Queensland, Queensland 4072, Australia, [§]Ludwig Institute for Cancer Research, P.O. Box 2008, Royal Melbourne Hospital, Victoria 3050, Australia, [#]These authors contributed equally.

ABSTRACT Understanding the interactions between drug carriers and cells is of importance to enhance the delivery of therapeutics. The release of therapeutics into different intracellular environments, such as the lysosomes or the cell cytoplasm, will impact their pharmacological activity. Herein, we investigate the intracellular fate of layer-by-layer (LbL)-assembled, submicrometer-sized polymer hydrogel capsules in a human colon cancer derived cell line, LIM1899. The cellular uptake of the disulfide-stabilized poly(methacrylic acid) (PMA_{SH}) capsules by colon cancer cells is a time-dependent process. Confocal laser scanning microscopy and transmission electron microscopy reveal that the internalized capsules are deformed in membrane-enclosed compartments, which further mature to late endosomes or lysosomes. We further demonstrate the utility of these redox-responsive PMA_{SH} capsules for the delivery of doxorubicin (DOX) to colon cancer cells. The DOX-loaded PMA_{SH} capsules demonstrate a 5000-fold enhanced cytotoxicity in cell viability studies compared to free DOX.

KEYWORDS: polymer capsules · endocytosis · intracellular fate · colorectal cancer · drug delivery

*Address correspondence to fcaruso@unimelb.edu.au, joan.heath@ludwig.edu.au.

Received for review January 27, 2010 and accepted April 16, 2010.

Published online April 26, 2010. 10.1021/nn100173h

Advanced drug delivery systems based on nanocarriers hold significant promise for improving cancer therapy outcomes.[1] There are currently over 10 nanotechnology-based anticancer products that have been approved for preclinical/clinical use, some showing favorable impact on the treatment of various cancers.[1,2] Among these first generation products, liposomal drug carriers and polymer−drug conjugates are the most dominant classes.[3] Recently, there has been increased interest in the potential of delivery vehicles formed by the layer-by-layer (LbL) technique as therapeutic carriers for controlled drug delivery.[4−6] Typically, these capsules are formed by deposition of interacting polymers onto a sacrificial colloidal template followed by dissolution of the core.[7] The assembly process allows for the manipulation of the properties of the capsules, including size, permeability, surface chemistry, surface functionality, and degradation characteristics.[4−6,8−11] Further, LbL-assembled capsules can be engineered to encapsulate a host of materials, including nucleic acids, peptides, proteins, and small drugs.[12−16]

Recently, we developed a novel LbL-assembled delivery system, which is based on the assembly of thiolated poly(methacrylic acid) (PMA_{SH}), to form hollow polymer hydrogel capsules.[17,18] The capsules are assembled by the alternate deposition of PMA_{SH} and poly(vinylpyrrolidone) (PVPON) onto silica particles, followed by subsequent cross-linking of the thiol groups (using an oxidizing agent such as chloramine-T) in the PMA_{SH} to form stable disulfide bonds and dissolution of the sacrificial silica core. The H-bonding interaction between PMA and PVPON is inherently unstable at physiological pH, and thus, when the capsules are placed in a pH 7 buffer, PVPON is expelled, resulting in single-component, disulfide cross-linked PMA_{SH} capsules. The disulfide-bonded capsules are stable in oxidizing conditions (such as the bloodstream) but disassemble in reducing environments such as the cytoplasm of the cell. We have demonstrated the potential of these capsules as a therapeutic delivery system for the *in vitro* and *in vivo* delivery of encapsulated proteins and peptides for vaccine applications,[13,16] as well as small molecule drugs for drug delivery to cancer cells.[14] The successful application of such capsules is highly dependent on their interaction with cells. Although studies using PMA_{SH} capsules have demonstrated that

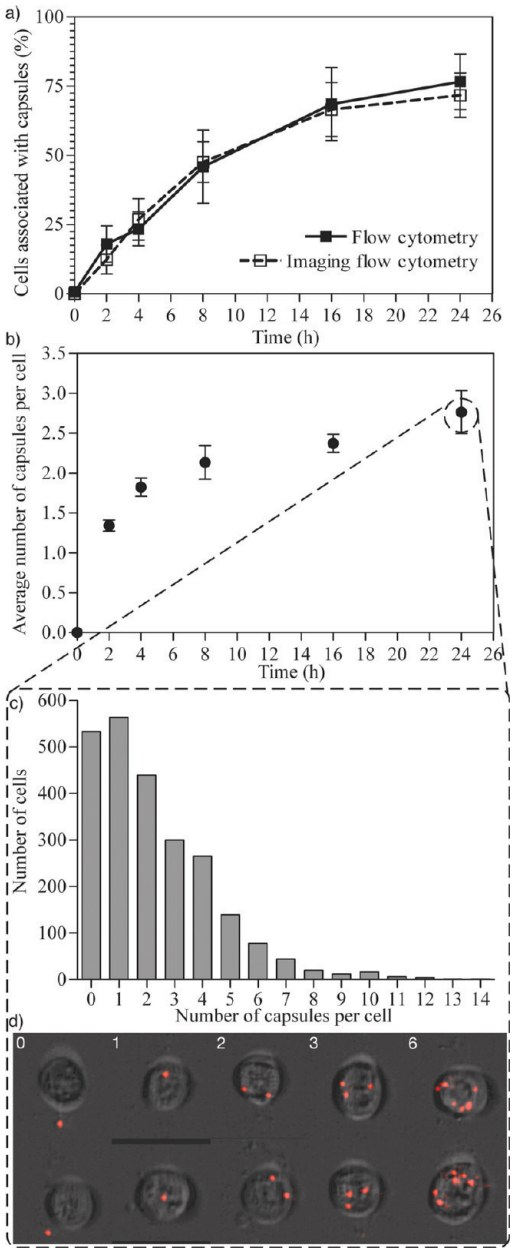

Figure 1. Time-dependent association of AF633-labeled PMA_{SH} capsules with LIM1899 cells over a 24 h incubation period at 37 °C, 5% CO_2. (a) Percentage of cells associated with PMA_{SH} capsules after incubation for various times was quantified by both flow cytometry and imaging flow cytometry. (b) Average number of PMA_{SH} capsules per cell that was associated with capsules, as evaluated by imaging flow cytometry. A representative experiment (24 h time point) is shown in the dotted-line frame. (c) Number of capsules in each analyzed cell. (d) Examples of association with cells detected by imaging flow cytometry. The numbers represent the number of internalized capsules. Data are the mean ± the standard error of three independent experiments; 20 000 cells were measured in each flow cytometry experiment, 5000 cells acquired, and only focused cells were analyzed in each imaging flow cytometry experiment.

the capsules can be internalized by several different cell types (*e.g.*, dendritic cells, monocytes, and colorectal cancer cells),[13,14,16] a detailed cellular uptake study, as well as the correlation of capsule uptake to effective therapeutic delivery, has not yet been performed.

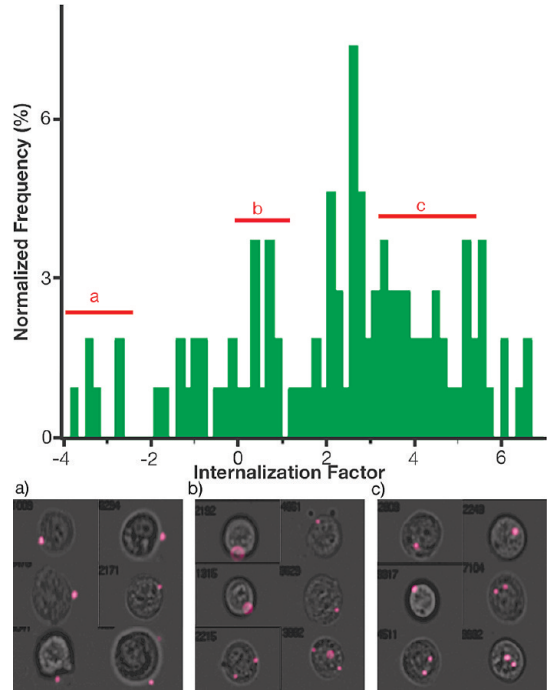

Figure 2. Quantification of the internalization of AF633-labeled PMA_{SH} capsules in LIM1899 cells by imaging flow cytometry. The cells were incubated with capsules at a capsule-to-cell ratio of 100:1 for 4 h at 37 °C, 5% CO_2. The degree of internalization is expressed as the internalization factor (IF). An overlay of the bright-field and fluorescence images of cells is shown for three representative areas: (a) capsules bound with cell membrane (negative IF); (b) capsules internalized within cells but in close proximity to the cell membrane (IF 0−1); (c) capsules internalized and trafficked within cells (IF >3).

Understanding the key processes of drug carrier internalization will form the basis of effective delivery. Studies have demonstrated that most polymeric nanocarriers are taken up by an endocytic process and that their uptake is both concentration- and time-dependent.[8,19−26] Recently, progress has been made in understanding the fate of polymeric nanocarriers once inside cells.[15,24,26−28] These studies indicate that, upon entry, nanocarriers are internalized into early endosomes created by the endocytic process. In some cases, these early endosomes then undergo a rapid maturation to late endosomes that are able to fuse with either other late endosomes or lysosomes.[15,24,26,27] In other cases, the internalized nanocarriers are able to escape from early endosomes and subsequently interact with other organelles inside the cell, such as the endoplasmic reticulum (ER) and the Golgi apparatus.[28] Studies on the cellular uptake of micrometer-sized (3 μm) polyelectrolyte capsules by tumor cells and dendritic cells have also shown that the uptake of the capsules involves endocytic processes in cells, and that the internalized capsules are localized and degraded in lysosomes.[15,24,26] However, the internalization process can vary dramatically among LbL-assembled capsules due to differences in composition, size, and charge of the capsules, as well as the cell physiology.

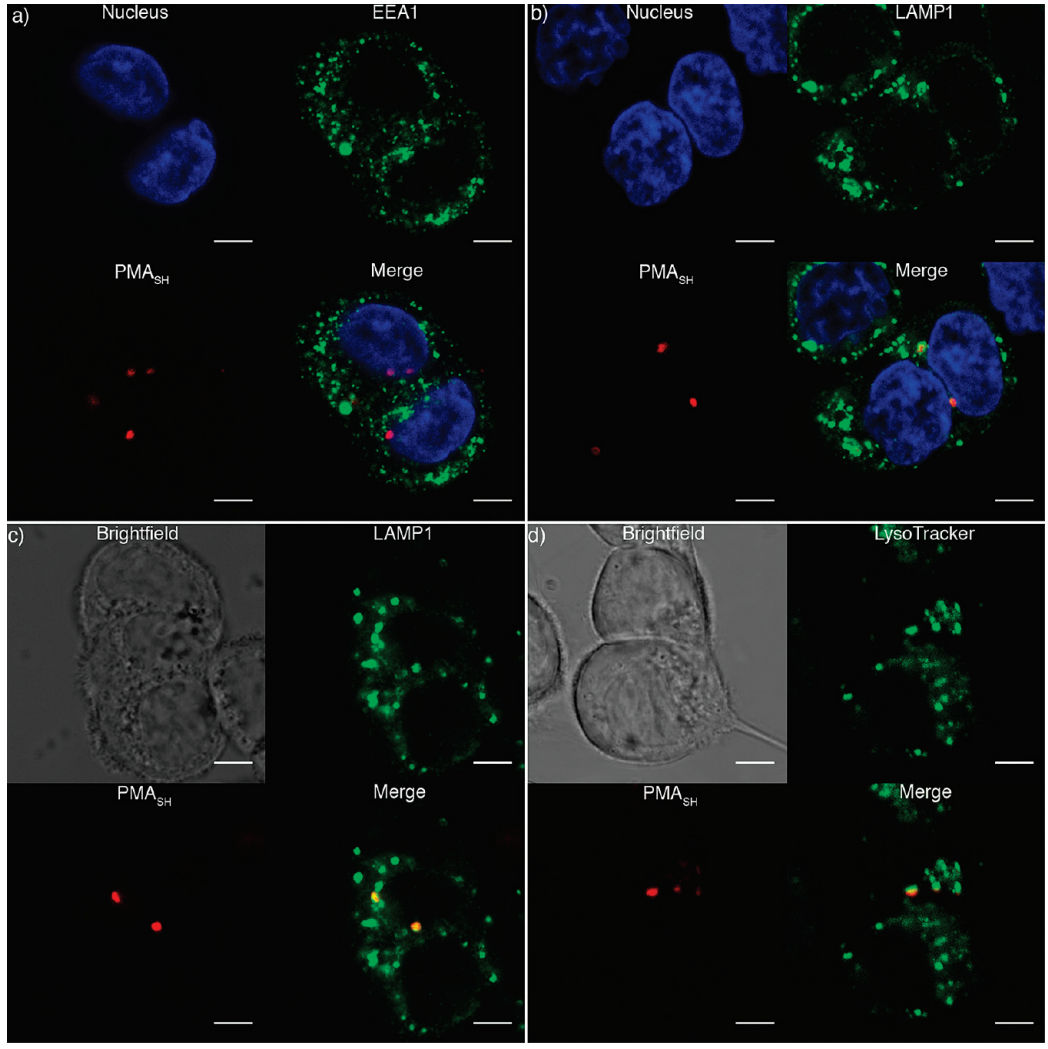

Figure 3. CLSM images of LIM1899 cells with internalized AF633-labeled PMA_{SH} capsules. Internalized AF633-labeled PMA_{SH} capsules (red) are colocalized with late endosomes and lysosomes, but not early endosomes, in LIM1899 cells. All cells were incubated with PMA_{SH} capsules for 24 h at 37 °C, 5% CO_2. Early endosomes were labeled with anti-EEA1 antibody (a, green), and late endosomes and lysosomes were immunostained with anti-LAMP1 antibody (b,c, green). Late endosomes and lysosomes were labeled with LysoTracker Blue (d, pseudocolored in green). In some samples, nuclei were counterstained with Hoechst 33342 (a,b, blue). Bright-field images of the cells are shown in gray (c,d). Scale bars = 5 μm.

Herein, we investigate the interactions between a human primary colorectal carcinoma derived cell line, LIM1899,[29] and PMA_{SH} capsules. The capsules used in this study were assembled on 585 nm silica particle templates, and due to the pH-responsive properties of PMA_{SH}, the final size of the capsules ranged from 600 nm (pH 4) to 850 nm (pH 8).[11,18] Our results indicate that the internalized capsules accumulate in the late endosome/lysosome compartments. Following the uptake of DOX-loaded PMA_{SH} capsules, we also observed a broad distribution of DOX in the cells, suggesting that the disulfide cross-linked capsules are deconstructed during intracellular trafficking, thereby leading to DOX release. Due to the lipophilic properties of the drug/oil emulsion studied, DOX appeared to partially diffuse through the endocytic vesicle membrane, resulting in cytotoxicity to the LIM1899 cells. The distribution of DOX within the cells was significantly different than the distribution obtained when free DOX was incubated with the cells and showed a 5000-fold increase in efficacy compared to free DOX.

RESULTS AND DISCUSSION

To examine the effect of the submicrometer-sized PMA_{SH} capsules on cell growth and viability, the potential cytotoxicity of PMA_{SH} capsules was measured by the reduction of MTT to formazan by metabolically active cells, which correlates with the number of viable cells.[30] LIM1899 cells show unchanged proliferation after incubation for 48 h with increasing doses of PMA_{SH} capsules up to 2×10^5 capsules μL^{-1} (a capsule to cell ratio of approximately 4000:1), suggesting that PMA_{SH} capsules are nontoxic in the concentration range studied (Figure S1, Supporting Information). The limited cytotoxicity of PMA_{SH} capsules supports their use as suitable drug delivery vehicles, which is in accordance with our previous studies using a different human cell line.[14]

We next monitored the interaction between Alexa Fluor 633-labeled (AF633-labeled) PMA_{SH} capsules and LIM1899 cells at a concentration of 2×10^4 capsules μL^{-1} (a capsule to cell ratio of approximately 100:1) as a function of time. The extent of association of LIM1899 cells with PMA_{SH} capsules was investigated over 2−24 h using flow cytometry, which showed that the interaction between PMA_{SH} capsules and cells is time-dependent (Figure 1). Significant association of cells with PMA_{SH} capsules is only apparent after several hours, with approximately 70% of cells associated with capsules after 24 h of incubation, suggesting slow binding and uptake of the PMA_{SH} capsules. The association and average number of the internalized PMA_{SH} capsules per cell were analyzed using imaging flow cytometry (IFC), which combines flow cytometry with fluorescence microscopy in a single platform. The images were acquired in extended depth of focus (EDF) mode, which provides focused 15 μm deep images of the cells and enables quantitative analysis of the entire cell. The association of capsules with cells was determined based on the images of individual cells, which allows exclusion of false positive events due to free capsules passing the detector concurrently with cells. In agreement with the flow cytometry analysis, IFC revealed a similar time-dependent interaction profile of PMA_{SH} capsules with the cells (Figure 1a). IFC also revealed that, among the cells that are associated with capsules, on average only 2−3 endocytic compartments containing capsules are present within each cell after 24 h incubation (Figure 1b), although some cells accumulate larger numbers (Figure 1c,d). The low binding and uptake of PMA_{SH} capsules are partly due to their negative surface charge at pH 7.4[8,18] because the outer surface of cells has a net negative charge.[31] This low nonspecific uptake provides a favorable framework to enhance the internalization in specific cells, for example, by the covalent attachment of a targeting ligand or antibody.[8]

To distinguish internalized capsules from the externally bound capsules, IFC was performed with a normal depth of field, which acquires a cross-sectional image of the cell with a 2 μm depth of focus. Combining the bright-field image of the cell with the fluorescent image of the capsule enables the internalization factor (IF) to be determined. A positive value for IF corresponds to a cell with internalized capsules, whereas a negative IF corresponds to surface-associated capsules. Cells were analyzed after 4 h incubation with capsules (capsule to cell ratio of 100:1) at 37 °C. Analysis at shorter incubation times was not possible due to the low number of cells associated with the capsules. As shown in Figure 2, about 80% of the cells with capsules bound had an IF greater than 0, suggesting that the majority of capsules are internalized soon after surface binding. The robustness of the IF as a measure of the degree of internalization was confirmed by analysis of cell images with different IFs. Cells with an IF less than

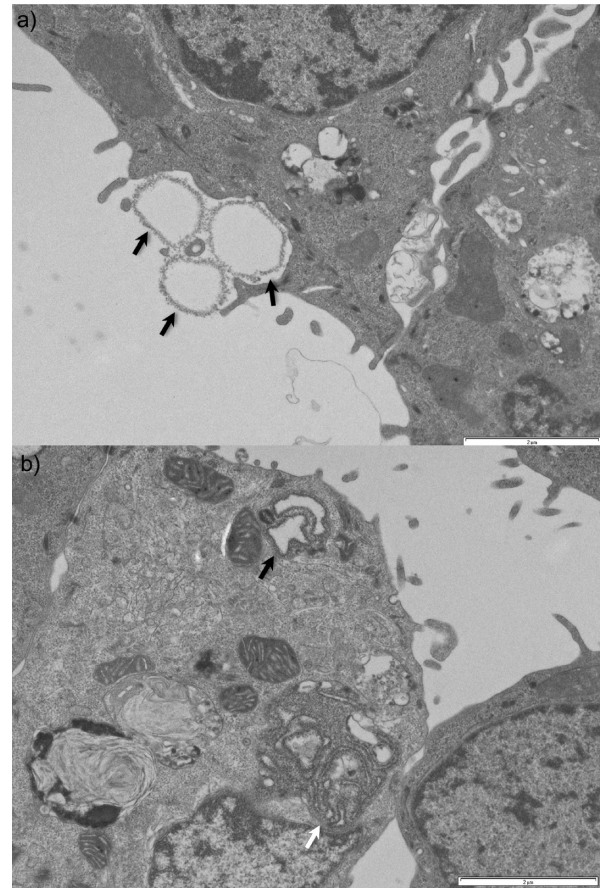

Figure 4. TEM images of LIM1899 cells that have internalized PMA_{SH} capsules. The cells were incubated with the capsules for 24 h at 37 °C, 5% CO_2. The TEM images suggest that the formation of plasma membrane protrusions is involved in the internalization of intact capsules (a, black arrows). Meanwhile, internalized capsules are found in membrane-enclosed electron-dense late endosomes or lysosomes (b, white arrow) and are deformed (b, black arrow). Scale bars = 2 μm. Images are representative of two separate experiments.

−3 (Figure 2a) clearly showed surface localization of the capsules, whereas cells with an IF greater than 3 (Figure 2c) demonstrated capsules inside the cell. Cells with an IF between 0 and 1 (Figure 2b) showed that the capsules were internalized by cells but were in close proximity to the cell membrane, suggesting capsules in the early stages of internalization.

Further insight into the internalization and intracellular distribution of PMA_{SH} capsules was gained by confocal laser scanning microscopy (CLSM) (Figure 3). LIM1899 cells were incubated with AF633-labeled PMA_{SH} capsules for 24 h at the same concentration (2×10^4 capsules μL^{-1}, a capsule to cell ratio of 100:1) used for the flow cytometry and image flow analyses. To visualize endocytic compartments, the cells were immunostained for early endosome antigen1 (EEA1) and the lysosome-associated membrane protein1 (LAMP1). The largely coiled-coil protein, EEA1, which acts as a Rab5 effector to mediate tethering and docking of early endosomes,[32] was used as a marker of early endocytic compartments. Meanwhile, LAMP1, which is an integral

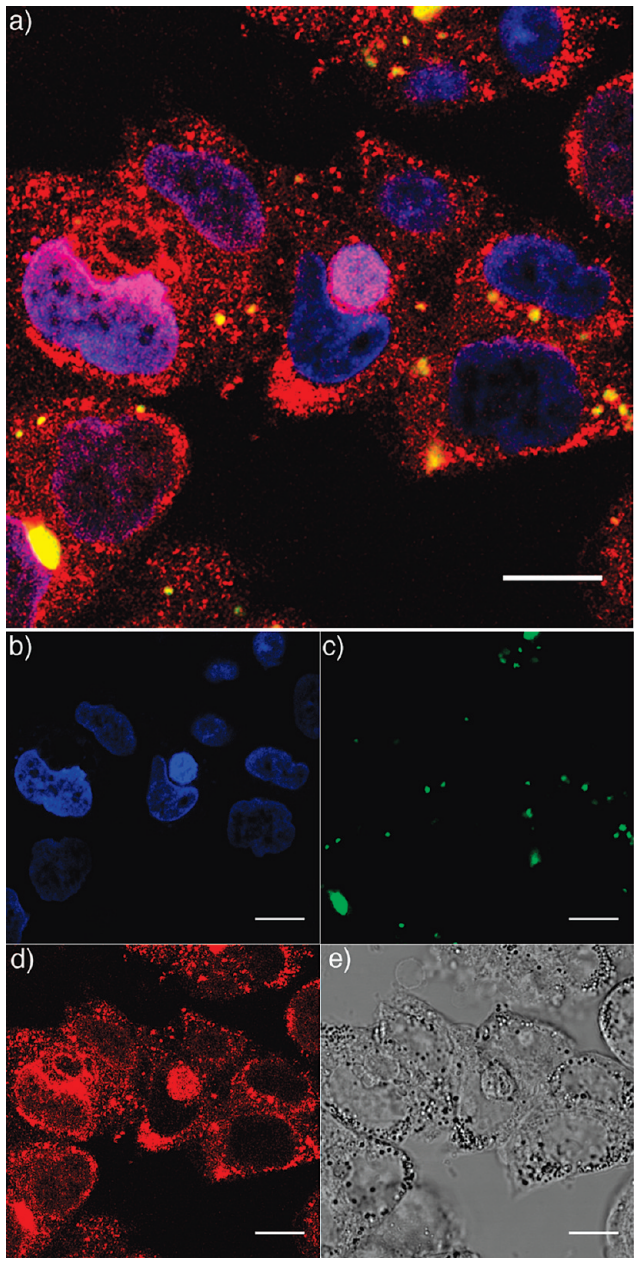

Figure 5. Encapsulated DOX is released from PMA_{SH} capsules after internalization of PMA_{SH}−DOX capsules by LIM1899 cells, as visualized by CLSM. Cells were treated with AF633-labeled PMA_{SH}−DOX (2×10^4 capsules μL^{-1}) at 37 °C, 5% CO_2 for 24 h. The nuclei were counterstained with Hoechst 33342 (b, blue). DOX (d, red) was released from the PMA_{SH} capsules (c, pseudocolored in green) and found in both the cytoplasm and nucleus (a, overlay). A bright-field image of the cells is shown in gray (e). Scale bars = 10 μm.

membrane protein with a highly N-glycosylated luminal domain, was used to identify the late endocytic compartments, specifically late endosomes and lysosomes.[33] CLSM images revealed that, after 24 h incubation, the majority of the internalized PMA_{SH} capsules are colocalized in the late endosomal/lysosomal compartments stained with LAMP1 (Figure 3b,c and Figure S2c,d in Supporting Information). By contrast, EEA1 immunostaining does not exhibit either significant overlap or close proximity with PMA_{SH} capsules (Figure 3a and Figure S2a,b). To confirm these results, LIM1899 cells were incubated with LysoTracker Blue, a marker for late endosomes and lysosomes based on their low internal pH. As shown in Figure 3d, the vesicles containing capsules are labeled with LysoTracker Blue (pseudocolored in green), suggesting that these vesicles are acidic. It was also noticeable that the majority of the internalized PMA_{SH} capsules are located in the perinuclear region of the cell, concentrated near the microtubule-organizing center where most of the fusion between late endosomal and/or lysosomal vesicles occurs.[34] Previous studies have reported that internalized PRINT (particle replication in nonwetting templates) particles move toward the nucleus in a time-dependent manner.[22] Taken together, these data suggest that the PMA_{SH} capsules are internalized into compartments which traffic to the juxtanuclear region, where they may fuse with late endosomes and lysosomes.

The intracellular distribution of PMA_{SH} capsules was also investigated by transmission electron microscopy (TEM). As shown in Figure 4a, the PMA_{SH} capsules outside of the cells were hollow and spherical with a thin, electron-dense wall. During the association of the capsules with the cell plasma membrane, the cell membrane extended over the capsules, forming cup-shaped invaginations. This suggests that macropinocytosis and/or phagocytosis may play a role in the uptake of the capsules. Within the cell, the capsules appeared in large membrane-enclosed compartments (diameter ~1 μm) with the morphology of late endosomes or lysosomes (Figure 4b). Cells cultured without capsules did not contain the membrane-bound structures found in the cells cultured with the capsules. It is notable that the capsules are deformed once they are internalized by cells, and more distorted capsules appear in late endosomes or lysosomes, which is consistent with other reports showing the high flexibility of the LbL-assembled capsules.[15,24] This result is also consistent with the intracellular fate of the capsules localizing in lysosomes identified using confocal microscopy (Figure 3).

The delivery of therapeutic complexes *via* endocytosis has important potential for improving cancer treatment. Several chemotherapeutics have been coupled to transferrin or folate due to the increased expression of their cognate receptors on malignant cells, leading to enhanced intracellular accumulation by receptor-mediated endocytosis and increased cytotoxicity in tumor cells compared to uncoupled drugs.[35] Similarly, nanoparticles may facilitate increased intracellular delivery as they can carry a large "payload". For example, a 70 nm nanoparticle can be loaded with up to ~2000 siRNA drug molecules, whereas antibody conjugates can accommodate less than 10.[1] To evaluate the potential of PMA_{SH} capsules as a carrier to deliver anticancer drugs, we incorporated DOX into the capsules using an oil-emulsion encapsulation strategy that we described

previously.[14] DOX has an intrinsic fluorescence spectrum (excitation at 480 nm, emission at 550−650 nm) that can be exploited to monitor localization of the drug. The amount of DOX loaded into the PMA_{SH} capsules was determined by back extraction into ethanol and measured by UV−vis spectrophotometry based on an absorbance calibration curve.[14] From these measurements, we calculated that the drug loading in each capsule was approximately 2.2×10^{-9} ng. The successful encapsulation of DOX was confirmed by the CLSM images of DOX-loaded AF633-labeled PMA_{SH} capsules (AF633-labeled PMA_{SH}−DOX), showing red DOX fluorescence within an AF633-labeled capsules (Figure S3, Supporting Information).

To investigate the fate of the encapsulated DOX, AF633-labeled PMA_{SH}−DOX capsules were added to the medium of adherent LIM1899 cells with continuous gentle shaking for 24 h in a humidified atmosphere at 37 °C, 5% CO_2. Cells were then rinsed with phosphate buffered saline (PBS), fixed, and the nuclei counterstained with Hoechst 33342. The resulting CLSM images (Figure 5) show the internalization of AF633-labeled PMA_{SH}−DOX capsules inside the cells. Although some DOX still appears to colocalize with PMA_{SH} capsules, strong DOX fluorescence is observed in both the cytoplasm and the nucleus, indicating release of DOX from the capsules after internalization. It has been reported that endocytic compartments may provide a reducing capacity sufficient to cleave disulfide bonds.[36,37] We expect that, upon internalization, the redox-responsive PMA_{SH}−DOX capsules are deformed within endosomes created by endocytosis. Thereafter, these vesicles traffic and mature to acidified compartments, where the DOX/oleic acid emulsion may be released from the carrier. Due to the lipophilic properties of the DOX/oleic acid emulsion, it appears that DOX partially diffuses through the endocytic vesicle membrane, resulting in cytotoxicity to the LIM1899 cells. The released DOX is diffusely distributed in the cytoplasm, and a further proportion of DOX is found in the nucleus. Presumably, a fraction of the DOX/oleic mixture released into the cytoplasm formed a DOX−proteasome complex, which may have been actively transported to the nucleus as a result of tagging with a nuclear localization signal presented in the proteasome, as reported previously.[38] Notably, DOX fluorescence in the cytoplasm is stronger than in the nucleus, in contrast to the findings obtained when cells are incubated with free DOX, where DOX is primarily localized to the nucleus (Figure 6). The different distribution of DOX in the cells after capsule internalization compared to that of free DOX suggests that encapsulated DOX enters cells *via* a different mechanism to free DOX. It also suggests that the PMA_{SH} capsules are stable in the presence of cells and serum-containing cell medium, achieving minimal premature release of DOX, as the rapid release of DOX in the extracellular environment would be expected to result in a nuclear distribution similar to that of free DOX. These data are consistent with our previous reports that disulfide-bonded PMA_{SH} capsules remain stable at pH 7.4 in the absence of reducing agents,[17] releasing negligible amounts of DOX from DOX/oleic acid loaded capsules at 37 °C over 24 h, as evaluated by both UV−vis absorbance measurements and MTT assays of the supernatant.[14]

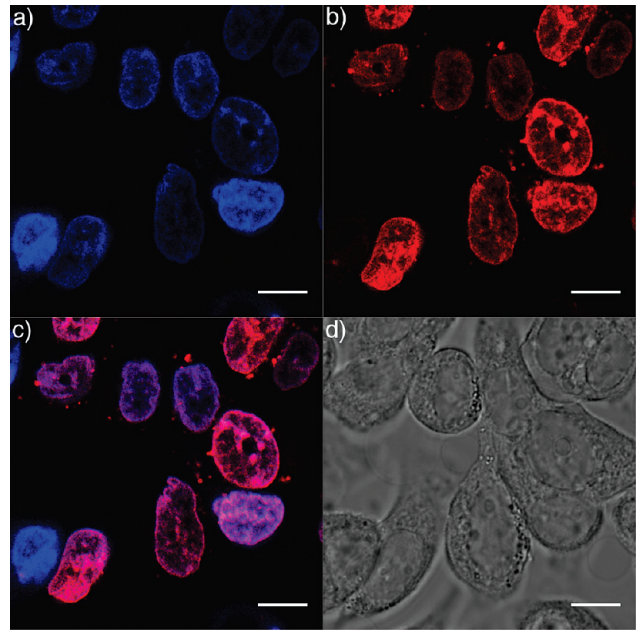

Figure 6. Free DOX accumulates in the nucleus of LIM1899 cells as visualized by CSLM (c, overlay). Cells were treated with DOX (1 μM) in growth media at 37 °C, 5% CO_2 for 24 h. The nuclei were counterstained with Hoechst 33342 (a, blue), and the intracellular distribution of DOX was visualized by confocal microscopy (b, red). Bright-field image of the cells is shown in gray (d). Scale bars = 10 μm.

The cytotoxicity of DOX-loaded PMA_{SH} (PMA_{SH}−DOX) capsules was evaluated on the LIM1899 cells using a colorimetric MTT assay. As shown in Figure 7a, cell viability was reduced in a dose-responsive manner when treated with DOX-loaded PMA_{SH} capsules (containing approximately 2.2×10^{-9} ng DOX per capsule) for 48 h at varying capsule to cell ratios. Importantly, oleic acid loaded PMA_{SH} capsules, used as a negative control, did not hinder cell growth compared to untreated cells, even at the highest concentration of PMA_{SH}−DOX capsules tested (Figure 7a, T2). This confirms that the cytotoxicity was due to delivery of the DOX and not the carrier system itself. On the basis of the amount of DOX in each capsule and the number of PMA_{SH}−DOX capsules used for each treatment, we calculated that the final concentration of DOX incubated with the cells was 8×10^{-4} nM (Figure 7a, T3), 8×10^{-3} nM (T4), and 8×10^{-2} nM (T5). Thus, this PMA_{SH}−DOX formulation showed up to a 5000-fold enhanced efficacy compared to free DOX (Figure 7b). Previously, we reported a significantly increased efficacy of cell killing (up to 10^6-fold) by DOX-loaded PMA_{SH} capsules in another colorectal carcinoma derived cell line, LIM1215. In that instance, the viability of the cells was measured by incubating the cells with the same dose of capsules

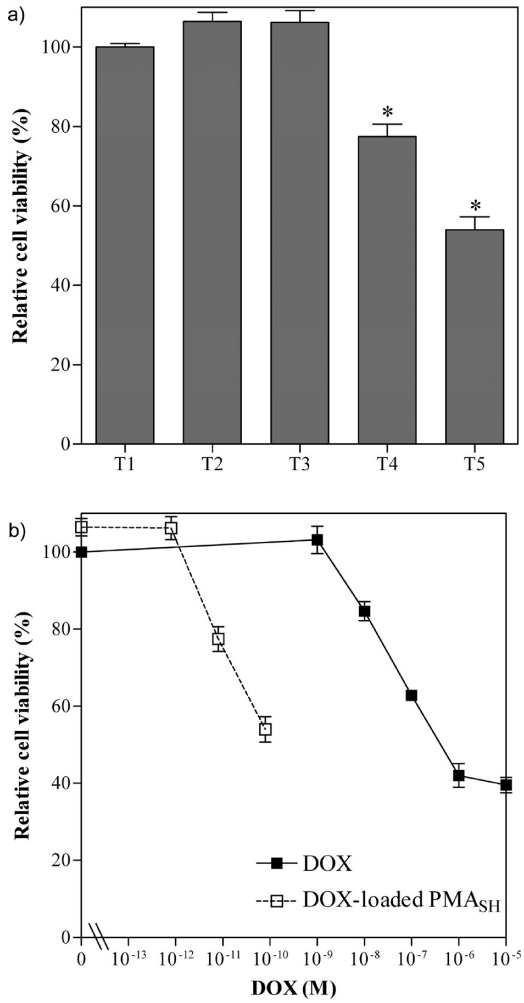

Figure 7. Enhanced cytotoxicity of DOX-loaded PMA$_{SH}$ capsules (compared to free DOX) on LIM1899 cells. Cells were treated for 48 h as follows. (a) T1, untreated cells; T2, oleic acid loaded PMA$_{SH}$ (2×10^4 capsules μL^{-1}); T3, DOX-loaded PMA$_{SH}$ (2×10^2 capsules μL^{-1}); T4, DOX-loaded PMA$_{SH}$ (2×10^3 capsules μL^{-1}); T5, DOX-loaded PMA$_{SH}$ (2×10^4 capsules μL^{-1}). (b) Comparison of therapeutic efficacy between DOX-loaded PMA$_{SH}$ and free DOX in LIM1899 cells. The values were normalized to that of untreated cells, which was set at 100%. Data are the mean ± the standard error of three independent experiments, each performed in triplicate. (*) $P < 0.001$ (one-way ANOVA coupled to Bonferroni multiple comparison test).

with different concentrations of encapsulated DOX for 24 h.[14] Although the calculated IC_{50} values are different between the two reports (most likely due to differences between the cell lines, periods of incubation, and dosage parameters), the considerably greater therapeutic effect achieved, compared to free DOX, is consistent. We propose that this enhanced cytotoxicity is due to the more effective intracellular accumulation of DOX, as the PMA$_{SH}$−DOX capsules are internalized by endocytosis, in contrast to free DOX, which enters cells by passive diffusion.[39] It has been reported that DOX causes both antiproliferative and cytotoxic effects in tumor cells through a number of mechanisms, including intercalation into DNA, interference with DNA unwinding and helicase activity, generation of free radicals, and direct membrane effects.[40] On the basis of the intracellular distribution of DOX from PMA$_{SH}$−DOX capsules and free DOX, it is expected that the major site of action for free DOX is the nucleus, while DOX from PMA$_{SH}$−DOX capsules may exert additional cytotoxic effects on other organelles through DNA-intercalation-independent mechanisms.

CONCLUSION

This paper provides the first detailed investigation of the cellular uptake and intracellular fate of submicrometer-sized polymer hydrogel PMA$_{SH}$ capsules. Our data reveal that these capsules associate with cells in a time-dependent manner. Subsequently, the internalized PMA$_{SH}$ capsules are distorted and accumulate in late endosomal or lysosomal compartments. Moreover, DOX-loaded PMA$_{SH}$ capsules are internalized by colorectal carcinoma derived cells, and the therapeutic release of DOX from the deconstructable PMA$_{SH}$ capsules is well supported by cell viability assays *in vitro*, which demonstrate significantly enhanced cell killing in response to DOX delivered by PMA$_{SH}$ capsules, compared to free DOX. This investigation assists in the evaluation and development of PMA$_{SH}$ capsules as a therapeutic delivery system, as understanding the key processes of capsule internalization will form the basis of effective delivery. In attempts to further increase the therapeutic efficacy, future studies will be aimed at functionalization of the PMA$_{SH}$ capsule surfaces with targeting ligands to promote their uptake and specificity of action. In addition, to broaden the applicability of these capsules to include the delivery of peptides, proteins, and siRNA molecules to the cytoplasm, strategies such as attachment of fusogenic peptides or cell-penetrating peptides may be used to facilitate the escape of PMA$_{SH}$ capsules from endocytic compartments.

METHODS

Materials: Silica particles (585 nm in diameter) were purchased from MicroParticles GmbH, Germany. Poly(methacrylic acid) (PMA; M_w 15 000 g mol^{-1}) was purchased from Polysciences, Inc. and was used as received. PMA$_{SH}$ with 15 mol % thiol groups was synthesized as described previously.[17] Bovine serum albumin (BSA), doxorubicin (DOX), oleic acid, and 3-[4,5-dimethylthiazol-2-yl]-2,5-diphenyltetrazolium bromide (MTT) were purchased from Sigma-Aldrich. Paraformaldehyde and glutaraldehyde were purchased from Electron Microscopy Sciences, USA. The mouse anti-human EEA1 and the mouse anti-human LAMP1 monoclonal antibodies were purchased from BD Biosciences Pharmingen, USA. AF488-labeled goat anti-mouse IgG antibody, Alexa Fluor 633 (AF633) maleimide, Hoechst 33342, and LysoTracker Blue were purchased from Invitogen, USA. The AF488-labeled huA33 mAb was produced at the Ludwig Institute for Cancer Research, Australia. High-purity water with resistivity greater than 18 MΩ · cm was obtained from a Millipore Rios/Synergy 2-stage system (Milli-Q water).

Cell Culture: The human colorectal carcinoma derived cell line, LIM1899, employed in this study has been described previ-

ously.[29] Cells were maintained in RPMI 1640 media (Gibco) containing 10% fetal bovine serum (FBS) and ADDS (10.8 μg mL^{-1} α-thioglycerol, 0.025 U mL insulin, 1 μg mL^{-1} hydrocortisone) at 37 °C in a humidified atmosphere containing 5% CO_2 and subcultured prior to confluence using trypsin/EDTA.

Preparation of PMA_{SH} Capsules and Their Loading with DOX: PMA_{SH} capsules were prepared as described previously.[17] Briefly, silica particles of 585 nm diameter were alternately incubated in solutions of PVPON or PMA_{SH} (1 g L^{-1}), resulting in a multilayered polymer film of $(PVPON/PMA_{SH})_5$/PVPON on the particles. Afterward, the particles were treated with a solution of chloramine T (2.5 mM) to achieve conversion of thiol groups into disulfide linkages between the PMA_{SH} layers, followed by removal of the silica core with aqueous hydrofluoric acid (5 M). The capsules were washed (×3) and resuspended in phosphate buffered saline (PBS), whereupon PVPON was released, resulting in single-component PMA_{SH} capsules. AF633-labeled PMA_{SH} capsules were prepared by mixing PMA_{SH} capsules with AF633 maleimide in 2-morpholinoethanesulfonic acid (MES) buffer (50 mM, pH 6) for 16 h under constant stirring at room temperature. The concentration of the capsules was determined by flow cytometry (Partec Cyflow Space, Germany) with absolute volume counting.

Loading of DOX in PMA_{SH} capsules was performed as described in detail elsewhere.[14] Briefly, PMA_{SH} capsules were dehydrated in ethanol and dispersed in a DOX/oleic acid mixture (50 μM) for 16 h at room temperature to allow infiltration of the oil phase through the semipermeable walls of the polymeric capsules, leading to filling of the capsules. The excess DOX/oleic acid mixture was removed by centrifugation and repetitive washing with PBS. The amount of DOX loaded into the PMA_{SH} capsules was determined following ethanol extraction from a UV−vis absorbance calibration curve.[14] DOX loading was found to be approximately 2.2×10^{-9} ng per capsule.

PMA_{SH}−Cell Interaction Profile Analysis: The percentage of cells associated with PMA_{SH} capsules and the average number of capsules per cell were assessed by both flow cytometry and imaging flow cytometry. For flow cytometry detection, 1×10^5 cells/well were seeded into 48-well plates and incubated (37 °C, 5% CO_2) with AF633-labeled capsules at a fixed concentration of 2×10^4 capsules μL^{-1}. At specified intervals (0, 2, 4, 8, 16, and 24 h), cells were washed (×3) with cold PBS and harvested by trypsinization followed by centrifugation at 400*g* for 5 min. The cell pellet was resuspended in PBS and analyzed by flow cytometry (Partec Cyflow Space). Cells (20 000 per analysis) were identified according to their scatter characteristics, and the percentage of cells associated with capsules was determined by acquisition of AF633 (FL5).

Samples for imaging flow cytometry analysis were prepared as described above except that 5000 cells were acquired for each time interval, and analysis was performed on focused cells only. The AF633 signal and corresponding bright-field image associated with individual cells were acquired on an ImageStream imaging flow cytometer (Amnis Corporation, Seattle) using the extended depth of field (EDF) collection mode. The data were analyzed using IDEAS software (Amnis Corporation, Seattle) to detect and enumerate capsules in each cell.

PMA_{SH} Capsule−Cell Internalization Analysis: Samples were prepared as described above. Briefly, the cells were treated with AF633-labeled capsules at a capsule-to-cell ratio of 100:1 at 37 °C for 4 h. The cells were then harvested and resuspended in PBS for imaging flow cytometry analysis. Images of 6000 cells and their fluorescence intensity (FL6) arising from associated capsules were acquired. The internalization analysis was performed on 100 cells, which were focused single cells associated with capsules. IDEAS software was used to create a cell mask based on the bright-field image of the cells, and the built-in internalization feature was used to calculate the degree of internalization.

Confocal Laser Scanning Microscopy (CLSM): Internalization experiments were performed using the same capsule dose as described above for the flow cytometry analysis (2×10^4 capsules μL^{-1}). LIM1899 cells were plated at 8×10^4 cells/well into 8-well Lab-Tek I chambered coverglass slides (Thermo Fisher Scientific, Rochester) and allowed to adhere overnight. Cells were then incubated with AF633-labeled PMA_{SH} capsules for 24 h (37 °C, 5% CO_2), followed by three washes with PBS. For experiments involving LysoTracker Blue, cells were further incubated with LysoTracker Blue (100 nM) in RPMI 1640 medium for 30 min at 37 °C. For experiments involving antibody immunostaining, cells were fixed with 4% paraformaldehyde for 20 min at room temperature (RT), permeabilized with 0.1% Triton X-100 in PBS for 1 min, and incubated with mouse anti-human EEA1 monoclonal antibody (2.5 μg mL^{-1} in PBS containing 0.25% BSA), or mouse anti-human LAMP1 monoclonal antibody (2.5 μg mL^{-1} in PBS containing 0.25% BSA) for 1 h at RT, followed by detection with AF488-labeled goat anti-mouse IgG (2 μg mL^{-1} in PBS containing 0.25% BSA) for 1 h at RT. Optical sections were collected with a Leica laser scanning confocal unit (TCS SP2; Leica, Germany). Colocalization analysis was performed with Imaris software (Bitplane AG, Switzerland).

Transmission Electron Microscopy (TEM): The intracellular fate of PMA_{SH} capsules was investigated with TEM using standard procedures. Briefly, LIM1899 cells were incubated with or without PMA_{SH} capsules (2×10^4 capsules μL^{-1}) for 24 h at 37 °C, 5% CO_2. After incubation, cells were fixed with 2.5% glutaraldehyde for 1 h at RT and washed (×3) with PBS. Samples were then dehydrated using a graded ethanol series followed by a Spurr's resin series. The cells were polymerized at 60 °C for 8 h, cut into ultrathin (80 nm) sections, loaded onto copper TEM grids, and stained with uranyl acetate and lead citrate prior to analysis by TEM (JEOL 1011, Japan). TEM images were obtained at an acceleration voltage of 60 kV. Cultures incubated with capsules were compared to cultures incubated without capsules.

Cell Viability Analysis by MTT Assay: Cell viability was measured by reduction of 3-[4,5-dimethylthiazol-2-yl]-2,5-diphenyltetrazolium bromide (MTT), as described previously.[30] Briefly, cells were seeded at 1×10^4 cells/well in 96-well plates and incubated with test substances for 48 h. After treatment, media were replaced by 200 μL of media containing MTT (0.5 mg mL^{-1}) and the cells incubated for a further 2 h. The resulting blue formazan was solubilized using 150 μL of acidified isopropanol (0.04 N HCl), and the absorbance at 560 nm was measured with a plate reader (Multiskan Ascent, Thermo Scientific). In the case of DOX-loaded PMA_{SH} capsules, the concentrations of DOX were calculated using the total amount of drug within the PMA_{SH} capsules divided by the volume of the treatment media. The reduction of MTT achieved by untreated cells was set at 100%, and that of test cells was expressed as a percentage of untreated cells. Data are shown as the mean ± the standard error for three independent experiments performed in triplicate.

Acknowledgment. This work was supported by the Australian Research Council under the Federation Fellowship (F.C.) and Discovery Project (F.C.) schemes and by National Health and Medical Research Council (NHMRC) Project Grant 433613 (J.K.H., F.C., E.C.N.) and Program Grant 487922 (J.K.H., F.C.). We gratefully acknowledge the assistance of Cameron Nowell (Centre for Advanced Microscopy, Ludwig Institute for Cancer Research, Melbourne) for helpful discussions regarding the confocal microscopy data.

Supporting Information Available: Assessment of biocompatibility of the capsules by MTT assay, 3D CLSM images of the intracellular fate of the capsules, and CLSM images of DOX-loaded PMA_{SH} capsules. This material is available free of charge *via* the Internet at http://pubs.acs.org.

REFERENCES AND NOTES

1. Heath, J. R.; Davis, M. E. Nanotechnology and Cancer. *Annu. Rev. Med.* **2008**, *59*, 251–265.
2. Wager, V.; Dullaart, A.; Bock, A. K.; Zweck, A. The Emerging Nanomedicine Landscape. *Nat. Biotechnol.* **2006**, *24*, 1211–1217.
3. Farokhzad, O. C.; Langer, R. Impact of Nanotechnology on Drug Delivery. *ACS Nano* **2009**, *3*, 16–20.
4. Johnston, A. P. R.; Cortez, C.; Angelatos, A. S.; Caruso, F. Layer-by-Layer Engineered Capsules and Their Applications. *Curr. Opin. Colloid Interface Sci.* **2006**, *11*, 203–209.
5. De Geest, B. G.; De Koker, S.; Sukhorukov, G. B.; Kreft, O.; Parak, W. J.; Skirtach, A. G.; Demeester, J.; De Smedt, S. C.; Hennink, W. E. Polyelectrolyte Microcapsules for Biomedical Applications. *Soft Matter* **2009**, *5*, 282–291.

6. Quinn, J. F.; Johnston, A. P. R.; Such, G. K.; Zelikin, A. N.; Caruso, F. Next Generation, Sequentially Assembled Ultrathin Films: Beyond Electrostatics. *Chem. Soc. Rev.* **2007**, *36*, 707–718.
7. Caruso, F.; Caruso, R. A.; Möhwald, H. Nanoengineering of Inorganic and Hybrid Hollow Sphere by Colloidal Templating. *Science* **1998**, *282*, 1111–1114.
8. Cortez, C.; Tomaskovic-Crook, E.; Johnston, A. P. R.; Scott, A. M.; Nice, E. C.; Heath, J. K.; Caruso, F. Influence of Size, Surface, Cell Line, and Kinetics Properties on the Specific Binding of A33 Antigen-Targeted Multilayered Particles and Capsules to Colorectal Cancer Cells. *ACS Nano* **2007**, *1*, 93–102.
9. Mar, Y.; Dong, W. F.; Hempenius, M. A.; Möhwald, H.; Vancso, G. J. Redox-Controlled Molecular Permeability of Composite-Wall Microcapsules. *Nat. Mater.* **2006**, *5*, 724–729.
10. Cortez, C.; Tomaskovic-Crook, E.; Johnston, A. P. R.; Radt, B.; Cody, S. H.; Scott, A. M.; Nice, E. C.; Heath, J. K.; Caruso, F. Targeting and Uptake of Multilayered Particles to Colorectal Cancer Cells. *Adv. Mater.* **2006**, *18*, 1998–2003.
11. Becker, A. L.; Zelikin, A. N.; Johnston, A. P. R.; Caruso, F. Tuning the Formation and Degradation of Layer-by-Layer Assembled Polymer Hydrogel Microcapsules. *Langmuir* **2009**, *25*, 14079–14085.
12. Zelikin, A. N.; Becker, A. L.; Johnston, A. P. R.; Wark, K. L.; Turatti, F.; Caruso, F. A General Approach for DNA Encapsulation in Degradable Polymer Microcapsules. *ACS Nano* **2007**, *1*, 63–69.
13. De Rose, R; Zelikin, A. N.; Johnston, A. P. R.; Sexton, A.; Chong, S.-F.; Cortez, C.; Mulholland, W.; Caruso, F.; Kent, S. J. Binding, Internalization, and Antigen Presentation of Vaccine-Loaded Nanoengineered Capsules in Blood. *Adv. Mater.* **2008**, *20*, 4698–4703.
14. Sivakumar, S.; Bansal, V.; Cortez, C.; Chong, S.-F.; Zelikin, A. N.; Caruso, F. Degradable, Surfactant-Free, Monodisperse Polymer-Encapsulated Emulsions as Anticancer Drug Carriers. *Adv. Mater.* **2009**, *21*, 1820–1824.
15. De Koker, S.; De Geest, B.; Singh, S. K.; De Rycke, Riet.; Naessens, T.; Van Kooyk, Y.; Demeester, J.; De Smedt, S. C.; Grooten. J. Polyelectrolyte Microcapsules as Antigen Delivery Vehicles to Dendritic Cells: Uptake, Processing, and Cross-Presentation of Encapsulated Antigens. *Angew. Chem., Int. Ed.* **2009**, *48*, 8485–8489.
16. Sexton, A.; Whitney, P. G.; Chong, S.-F.; Zelikin, A. N.; Johnston, A. P. R.; De Rose, R.; Brooks, A. G.; Caruso, F.; Kent, S. J. A Protective Vaccine Delivery System for *In Vivo* T Cell Stimulation Using Nanoengineered Polymer Hydrogel Capsules. *ACS Nano* **2009**, *3*, 3391–3400.
17. Zelikin, A. N.; Quinn, J. F.; Caruso, F. Disulfide Cross-Linked Polymer Capsules: *En Route* to Biodeconstructible Systems. *Biomacromolecules* **2006**, *7*, 27–30.
18. Zelikin, A. N.; Li, Q.; Caruso, F. Disulfide-Stabilized Poly(methacrylic acid) Capsules: Formation, Cross-Linking, and Degradation Behavior. *Chem. Mater.* **2008**, *20*, 2655–2661.
19. Panyam, J.; Zhou, W. Z.; Praba, S.; Sahoo, S. K.; Labhasetwar, V. Rapid Endo-Lysosomal Escape of Poly(DL-lactide-*co*-glycolide) Nanoparticles: Implications for Drug and Gene Delivery. *FASEB J.* **2002**, *16*, 1217–1226.
20. Panyam, J.; Labhasetwar, V. Biodegradable Nanoparticles for Drug and Gene Delivery to Cells and Tissue. *Adv. Drug Delivery Rev.* **2003**, *55*, 329–347.
21. Muro, S.; Cui, X.; Gajewski, C.; Murciano, J. C.; Muzykantov, V. R.; Koval, M. Slow Intracellular Trafficking of Catalase Nanoparticles Targeted to ICAM-1 Protects Endothelial Cells from Oxidative Stress. *Am. J. Physiol. Cell Physiol.* **2003**, *285*, C1339–C1347.
22. Gratton, S. E.; Ropp, P. A.; Pohlhaus, P. D.; Luft, J. C.; Madden, V. J.; Napier, M. E.; DeSimone, J. M. The Effect of Particle Design on Cellular Internalization Pathways. *Proc. Natl. Acad. Sci. U.S.A.* **2008**, *105*, 11613–11618.
23. Douglas, K. L.; Piccirillo, C. A.; Tabrizian, M. Cell Line-Dependent Internalization Pathways and Intracellular Trafficking Determine Transfection Efficiency of Nanoparticle Vectors. *Eur. J. Pharm. Biopharm.* **2008**, *68*, 676–687.
24. Javier, A. M.; Kreft, O.; Semmling, M.; Kempter, S.; Skirtach, A. G.; Bruns, O. T.; Del Pino, P.; Bedard, M. F.; Rädler, J.; Kas, J.; Plank, C.; Sukhorukov, G. B.; Parak, W. J. Uptake of Colloidal Polyelectrolyte-Coated Particles and Polyelectrolyte Multilayer Capsules by Living Cells. *Adv. Mater.* **2008**, *20*, 4281–4287.
25. Reibetanz, U.; Halozan, D.; Brumen, M.; Donath, E. Flow Cytometry of HEK 293T Cells Interacting with Polyelectrolyte Multilayer Capsules Containing Fluorescein-Labeled Poly(acrylic acid) as a pH Sensor. *Biomacromolecules* **2007**, *8*, 1927–1933.
26. De Geest, B. G.; Vandenbroucke, R. E.; Guenther, A. M.; Sukhorukov, G. B.; Hennink, W. E.; Sanders, N. N.; Demeester, J.; De Smedt, S. C. Intracellularly Degradable Polyelectrolyte Microcapsules. *Adv. Mater.* **2006**, *18*, 1005–1009.
27. Nam, H. Y.; Kwon, S. M.; Chung, H.; Lee, S. Y.; Kwon, S. H.; Jeon, H.; Kim, Y.; Park, J. H.; Kim, J.; Her, S.; Oh, Y. K.; Kwon, I. C.; Kim, K.; Jeong, S. Y. Cellular Uptake Mechanism and Intracellular Fate of Hydrophobically Modified Glycol Chitosan Nanoparticles. *J. Controlled Release* **2009**, *135*, 259–267.
28. Cartiera, M. S.; Johnson, K. M.; Rajendran, V.; Caplan, M. J.; Saltzman, W. M. The Uptake and Intracellular Fate of PLGA Nanoparticles in Epithelial Cells. *Biomaterials* **2009**, *30*, 2790–2798.
29. Andrew, S. M.; Teh, J. G.; Johnstone, R. W.; Russell, S. M.; Whitehead, R. H.; McKenzie, I. F.; Pietersz, G. A. Tumor Localization by Combinations of Monoclonal Antibodies in a New Human Colon Carcinoma Cell Line (LIM1899). *Cancer Res.* **1990**, *50*, 5225–5230.
30. Mosmann, T. Rapid Colorimetric Assay for Cellular Growth and Survival: Application to Proliferation and Cytotoxicity Assays. *J. Immunol. Methods* **1983**, *65*, 55–63.
31. Sherbet, G. V.; Lakshimi, M. S.; Rao, K. V. Characterisation of Ionogenic Groups and Estimation of the Net Negative Electric Charge on the Surface of Cells Using Natural pH Gradients. *Exp. Cell Res.* **1972**, *70*, 113–123.
32. Christoforidis, S.; McBride, H. M.; Burgoyne, R. D.; Zerial, M. The Rab5 Effector EEA1 Is a Core Component of Endosome Docking. *Nature* **1999**, *397*, 621–625.
33. Eskelinen, E. L.; Tanaka, Y.; Saftig, P. At the Acidic Edge: Emerging Functions for Lysosomal Membrane Proteins. *Trends Cell Biol.* **2003**, *13*, 137–145.
34. Luzio, J. P.; Pryor, P. R.; Bright, N. A. Lysosomes: Fusion and Function. *Nat. Rev. Mol. Cell Biol.* **2007**, *8*, 622–632.
35. Daniel, T. R.; Delgada, T.; Helguera, G.; Penichet, M. L. The Transferrin Receptor Part II: Targeted Delivery of Therapeutic Agents into Cancer Cells. *Clin. Immunol.* **2006**, *121*, 159–176.
36. Yang, J.; Chen, H.; Vlahov, I. R.; Cheng, J. X.; Low, P. S. Evaluation of Disulfide Reduction During Receptor-Mediated Endocytosis by Using FRET Imaging. *Proc. Natl. Acad. Sci. U.S.A.* **2006**, *103*, 13872–13877.
37. Saito, G.; Swanson, J. A.; Lee, K. D. Drug Delivery Strategy Utilizing Conjugation *via* Reversible Disulfide Linkages: Role and Site of Cellular Reducing Activities. *Adv. Drug Delivery Rev.* **2003**, *55*, 199–215.
38. Kiyomiya, K.; Matsuo, S.; Kurebe, M. Mechanism of Specific Nuclear Transport of Adriamycin: The Mode of Nuclear Translocation of Adriamycin-Proteasome Complex. *Cancer Res.* **2001**, *61*, 2467–2471.
39. Skovsgaard, T.; Nissen, N. I. Membrane Transport of Anthracyclines. *Pharmacol. Ther.* **1982**, *18*, 293–311.
40. Minotti, G.; Menna, P.; Salvatorelli, E.; Cairo, G.; Gianni, L. Anthracyclines: Molecular Advances and Pharmacologic Developments in Antitumor Activity and Cardiotoxicity. *Pharmacol. Rev.* **2004**, *56*, 185–229.